# ABraytCSPfuture

**Air-Brayton Cycle Concentrated Solar Power future** plants via redox oxides-based structured thermochemical heat exchangers / thermal boosters

# Deliverable D3.3.

# Optimized redox oxide formulations and structured objects for proof-of-concept-scale unit

## Dissemination Level: SEN

**WP3 Preparation of lab-scale redox oxides porous structured test specimens and application-specific testing**

Date: 21.02.2025

https://www.abraytcspfuture.eu/

*This project has received funding from the European Union's Horizon Europe research and innovation programme under grant agreement no 101084569.*

# Disclaimer

The work described in this document has been conducted within the ABraytCSPfuture project that is co-funded by the European Union. Views and opinions expressed herein are however those of the author(s) only and do not necessarily reflect those of the European Union or of the granting authority, European Climate, Infrastructure and Environment Executive Agency (CINEA). Neither the European Union nor the granting authority can be held responsible for them.

| **Grant Agreement Number: 101084569 Acronym: ABraytCSPfuture** | | | | |
|---|---|---|---|---|
| **Full Title** | **A**ir-**Brayt**on Cycle **C**oncentrated **S**olar **P**ower **future** plants via redox oxides-based structured thermochemical heat exchangers/thermal boosters | | | |
| **Call Topic Identifier:** | HORIZON-CL5-2021-D3-03 | | | |
| **Funding Scheme** | HORIZON EUROPE, RIA – Research and Innovation Actions | | | |
| **Project start date:** | 01.11.2022 | | | |
| **Project duration:** | 48 months | | | |
| **Project URL** | https://www.abraytcspfuture.eu/ | | | |
| **EU Project Officer** | Clara Astudillo Llorente | | | |
| **Project Coordinator** | DLR – German Aerospace Center | | | |
| **Deliverable** | D3.3 – Optimized redox oxide formulations & structured objects for proof-of-concept-scale unit | | | |
| **Date of Delivery** | Contractual | 31.01.2025 | Actual | 21.02.2025 |
| **Nature** | Report | | | |
| **Dissemination Level** | Sensitive | | | |
| **Lead Beneficiary** | CERTH | | | |
| **Document History** | | | | |

| **Version** | **Issue Date** | **Change History** | **Authors** | **Organisation** |
|---|---|---|---|---|
| 1.0 | 20.01.2025 | Document drafted | G. Karagiannakis, C. Pagkoura | CERTH |
| 1.1 | 10.02.2025 | Updated with final partner feedback | C. Agrafiotis, D. Vellas, A. Eltayeb, M. Pein, C. Pagkoura, G. Karagiannakis, N. Hornskov, L. Yuan, J. Marcher | DLR, CERTH, LET |
| 1.2 | 20.02.2025 | Final Review | S. Herrero, I. Muñoz | TEKN |

# About the Project

*ABraytCSPfuture* sets forth an innovative, carbon-neutral way for implementing the highly efficient air-Brayton gas turbine power generation cycles into future air-operated Concentrated Solar Power (CSP) plants. Air-Brayton cycles are used in traditional power plants where, however, involve fossil fuels combustion via pressurized air. *ABraytCSPfuture*'s carbon-neutral approach aims at achieving higher solar-to-electricity efficiencies, vital for competitiveness of CSP and non-reachable by either PVs or molten salts and thermal oils, increasing in parallel significantly the plants' storage capability. The project will develop and demonstrate a first-of-its-kind compact, dual-bed thermochemical reactor/heat exchanger unit that will transfer heat from a non-pressurised air stream to a pressurised one, while also operating as a thermal booster, raising the temperature of the pressurized stream to the level required for Brayton cycles. Furthermore, the volumetric solar energy storage density of air-operated CSP plants will be significantly increased by rendering their current sensible-only regenerative storage systems to hybrid sensible-thermochemical storage ones within the same storage volume. Both these functionalities will be materialized by thermochemical reactor/heat exchanger units comprised of non-moving, flow-through porous ceramic structures (honeycombs or foams) based on earth-abundant, cost-efficient, non-toxic oxide materials and exploiting reversible reduction/oxidation reactions of such oxides in direct contact with air, accompanied by significant endothermic/exothermic heat effects. The proposed technology is set forth by an interdisciplinary partnership spanning the entire CSP value chain, comprised of leading research centres, universities, innovative SMEs and large enterprises, including ancillary services providers and technology end-users.

| | | |
|---|---|---|
| Deutsches Zentrum fuer Luft- und Raumfahrt e.V., **DLR** | DE | DLR |
| Centre for Research & Technology Hellas, **CERTH** | EL | CERTH CENTRE FOR RESEARCH & TECHNOLOGY HELLAS |
| University of Twente, **UT** | NL | UNIVERSITY OF TWENTE. |
| Fundación CENER, **CENER** | ES | CENER NATIONAL RENEWABLE ENERGY CENTRE ADItech |
| Fundación TEKNIKER, **TEKN** | ES | Tekniker |
| Fraunhofer Gesellschaft zur Foerderung der angewandten Forschung e.V., **FHG (IWKS)** | DE | Fraunhofer IWKS |
| OPRA Turbines, **OPRA** | NL | Destinus |
| KRAFTBLOCK GmbH, **KB** | DE | KRAFT BLOCK |
| LANDSON Emission Technologies A/S, **LET** | DK | landson |
| COBRA Instalaciones y Servicios S.A., **COBRA** | ES | cobra |

# Table of Contents

*This deliverable is part of a project that has received funding from the European Union's Horizon Europe research and innovation programme under grant agreement no 101084569*

# Executive Summary

The deliverable capitalizes on findings and results of submitted deliverables D3.1, D3.2 and to a lesser extent D7.1 as well as past submitted deliverables of WP2 to conclude with the chosen/optimum material composition and structure combination that will constitute the primary building block of the proof-of-concept scale unit to be developed in WP5. The consolidated results and analysis point clearly towards the **$Ca_{0.90}Sr_{0.10}MnO_3$ (CS10MO) perovskite** shaped by extrusion into a honeycomb geometry that will have a relatively high bulk density (e.g. > 1.2 $kg \cdot L^{-1}$ and preferably as close as possible to 2 $kg \cdot L^{-1}$) so that the energy density potential will be appreciable and in particular exceeding the targeted value of 300 $kWh \cdot m^{-3}$ for the pre-defined 300-1100°C operating temperature range of the storage system.

Currently available scaled-up extrusion capabilities at LET and a preliminary qualified strategy are briefly stated here. Moreover, the final geometry – to be used as the starting point of the relevant developmental work – is chosen. If needed and depending on the outcome of extrusion/calcination and first experimental energetic and structural stability studies with small-scale specimens sectioned from those in the frame of WP3, another tool/die able to provide a slightly modified geometry may need to be eventually chosen.

# Changes with respect to the DoA

There are no notable changes referring to the DoA and thus the timely preparation of the present deliverable, implementation of the workplan of WP3 as well as the necessary anticipated conclusions and feedback to continue the work in the project as a whole, until submission of this deliverable, have not been affected.

# 1. Introduction

This deliverable refers directly to the final shortlisting of optimized redox oxide formulations and shape/characteristics of structured objects for the proof-of-concept scale unit and operating conditions maximizing exploitation of materials' properties, determined from thermochemical and microstructural characterization of porous specimens. Most of the work presented herein was in the framework of WP3/Task 3.4, while most of the necessary input to end up with the shortlist is directly obtained from Tasks 3.1-3.3 and thus submitted deliverables D3.1 and D3.2. References to those deliverables are frequently made in the text. Secondarily and as an important addition to ensure that the decision is made on the basis of an integrated and holistic approach, scaling-up feasibility perspectives, preliminary environmental/financial aspects already identified by WP7 (deliverable D7.1) and elements from the main outcome of WP2 so far are also taken into account.

# 2. Choice of composition and structure geometry combination

A number of important criteria, as stated and analysed below based on project findings (WP3 and beyond), are considered for the choice of the optimized targeted building block of the prototype system to be constructed and operated (WP5, WP6). Parameters like main performance indicators, scaled-up manufacturing feasibility and environmental/ financial aspects are reviewed and the decision is made by examining how well the available options perform with respect to those parameters/criteria.

## 2.1 Overall assessment regarding important thermophysical and thermochemical characteristics

The specific heat capacity, the calculated thermochemical energy density and the bulk/envelope density of structures (both redox and sensible-only) are of fundamental importance in the sense that they collectively define the total energy storage density potential of the ABCSPF's concept. Table 1 provides an overview of these parameters, all of them measured directly experimentally or calculated based on experimental data. Table 2 summarizes the final calculated energy densities as well as the heat exchange efficiency per structure. The latter is the % of total heat transferred from the structure to the air flow, as defined by the ratio of the two calculated energies, in the course of the exothermal oxidation reaction (discharge step) and should only be accounted for to identify the trend between the 3 structures rather than in terms of its absolute values which are anyway low in all cases because the structures are very small (i.e. high surface to volume ratio) and thus characterized by high heat losses.

| Structure/composition description | Bulk density ($g \cdot cm^{-3}$) | Specific heat capacity – Cp ($J \cdot g^{-1} \cdot K^{-1}$) / indicative average value 300-1100°C | Thermochemical energy density ($J \cdot g^{-1}$) |
|---|---|---|---|
| **111 cpsi CMO honeycomb** | 1.20 | 1.21 | **243 ± 18** |
| **59 cpsi CMO honeycomb** | 2.25 | 1.21 | **350 ± 45** |
| **60 ppi CS10MO foam** | 0.81 | 1.27 | **530 ± 15** |
| **59 cpsi CS10MO honeycomb** | 2.10 | 1.27 | **480 ± 5** |

**Table 1:** Main parameters directly affecting the energetic performance of structures studied so far (as measured in WP3 and reported in D3.1 and D3.2)

| Structure/composition description | Total energy density ($J \cdot g^{-1}$) | Total volumetric energy density ($kWh \cdot m^{-3}$) | Heat exchange efficiency (%) |
|---|---|---|---|
| **111 cpsi CMO honeycomb** | 1215 | 405 | 32 |
| **59 cpsi CMO honeycomb** | 1280 | 800 | 22 |
| **60 ppi CS10MO foam** | 1555 | 350 | 50 |
| **59 cpsi CS10MO honeycomb** | 1440 | 840 | 28 |

**Table 2:** Overview of energy storage density calculated based on the values reported in Table 1 (as also reported in D3.2)

Overall, the 59 cpsi honeycomb geometry possesses a clear advantage, especially in terms of its volumetric energy density which is primarily attributed to the high bulk/envelope density of this particular structure. In terms of total mass energy density, differences among the different structures are not profound but the one made of the CS10MO composition are measurably better.

## 2.2 Overall assessment regarding structural (macro- and micro-) aspects

In addition to the important aspects relating to the energy density potential of the candidate building blocks of the storage system, it is also of fundamental importance that the chosen structure(s) must be robust enough to withstand the challenging conditions of the operational requirements of the ABCSPF's application. To summarize, these include:

- The constant heating/cooling as required by the defined broad operational window of 300-1100$^{o}$C.
- The potential changes involved in the course of the operation within the aforementioned temperature range, including the redox scheme. The latter involves the constant removal and incorporation of oxygen (''breathe-out, breathe-in'') in the materials' lattice which anyway introduces stresses. Potential changes in the crystal structure, either major or secondary, introduce additional stresses that, as identified in the past [1] and also addressed in deliverables of WP2 and D3.2, may also be of a detrimental nature to the structures undergoing multi-cyclic operation.
- The thermal shock induced by the abrupt oxidation of the structure. As demonstrated in D3.2, the sudden oxidation results to an abrupt temperature increase on the surface of the structure that locally can exceed even 200$^{o}$C under certain conditions. This, especially when repeated hundreds or thousands of times, may endanger the integrity of the structures and lead to extensive cracking.

The effect of all the above challenges is assessed via a combination of macroscopic and microscopic (i.e. via Scanning Electron Microscopy – SEM) observations as well as comparative compressive crushing strength measurements of pristine and cycled/used structures. The former are very informative on the phenomena and main characteristics of the mechanism of the abovementioned effects while the latter constitute a final quantitative confirmation of the assessment made by the comprehensive observations. By the time of submission of the present deliverable, only measurements on pristine structures have been completed and these have clearly shown that the extruded redox honeycombs have 10-25 times higher crushing strength than the respective foams calcined at the same temperature. Thus, at least when referring to pristine structures, honeycomb formulations have a clear advantage. During the next months, emphasis will be put on producing structures subjected to a variable number of cycles to assess the evolution of crushing strength with the number of operational redox/thermal cycles, while a relevant measurement on the 59 cpsi CS10MO honeycomb has already been scheduled for end of M29 (see D3.2).

Table 3 below provides an overview of macroscopic and microscopic observations for all 4 structures evaluated so far. This is based on relevant images and photographs and relevant analysis already included either in the submitted deliverable D3.2 or in the 1$^{st}$ periodic technical report.

| Structure/ composition description | Main macroscopic observations (used/cycled samples) | Main microscopic (SEM) observations (used samples and/or used vs pristine) |
|---|---|---|
| **111 cpsi CMO honeycomb*** (72 cycles)<br>**59 cpsi CMO honeycomb*** (80 cycles) | - Several **visible cracks** in cycled structures before removal from reactor holder.<br>- **No visible swelling or elongation** of structures.<br>- Structures destroyed (broke into pieces) in the process of removal from the reactor holder. | - **Micro-cracks** evident in both low & higher magnification images.<br>- **Changes in the texture of grains' surface** vs the pristine structure visible in the high magnification images; i.e. plated/rough vs smooth.<br>- Changes **attributed to cyclic orthorhombic-cubic** structural transition during thermal cycles |
| **60 ppi CS10MO foam** (214 cycles) | - **No visible cracks** in cycled structures before removal from reactor holder.<br>- **No visible swelling or elongation** of structure.<br>- Minor damage in the process of removal from the reactor holder (a few pieces detached). **OK to assess dimensional changes**, which were not measurable. | - **Only grains sintering** phenomena visible.<br>- **Sparse minor micro-cracks** detected<br>- Difference vs CMO structures (see above) attributed to the **suppression of ortho-cubic** structural transition by Sr-doping<br>- **No compositional changes** vs pristine structure (EDS) |
| **59 cpsi CS10MO honeycomb** (203 cycles) | - **No visible cracks** in cycled structures before removal from reactor holder.<br>- **No visible swelling or elongation** of structure.<br>- No visible damage in the process of removal from the reactor holder (**removed intact**). OK to assess dimensional changes, which were **tolerable**: **+ 2.2% in diameter; + 1.8% in length**. | - SEM analysis pending (scheduled for end of M29) |

**Table 3:** Overview of macroscopic observations referring to the robustness/thermomechanical stability of redox structures studied so far. **observations for the two CMO honeycomb were essentially identical and are thus stated here together*

Based on the above, CS10MO composition brings a clear advantage. A thicker structure (i.e. 59 cpsi honeycomb) also enhances robustness. Further analyses and measurements are underway.

## 2.3 Overall assessment based on scaled-up manufacturing feasibility

### 2.3.1 All-redox foams

Attempts to scale-up the manufacturing of foam-like structures were led by DLR. It is reminded here that successfully prepared small-scale structures (see deliverable D3.1) have a diameter of up to approx. 65 mm after sintering (with a PU template of Ø80 mm). Scaling-up attempts followed, targeted at foams with a final diameter of about 120 mm (i.e. 135 mm for initial PU foam) by simply using lager size PU-foam templates and adjusting the coating protocol to properly and homogeneously impregnate the sacrificial template with the redox material slurry. A representative outcome of such attempts is depicted in Figure 1, which photographs of representative larger foam structures after impregnation of the respective PU templates and after calcination at 1300°C using the same protocol under which the smaller 24 mm diameter size foams were sintered, are provided.

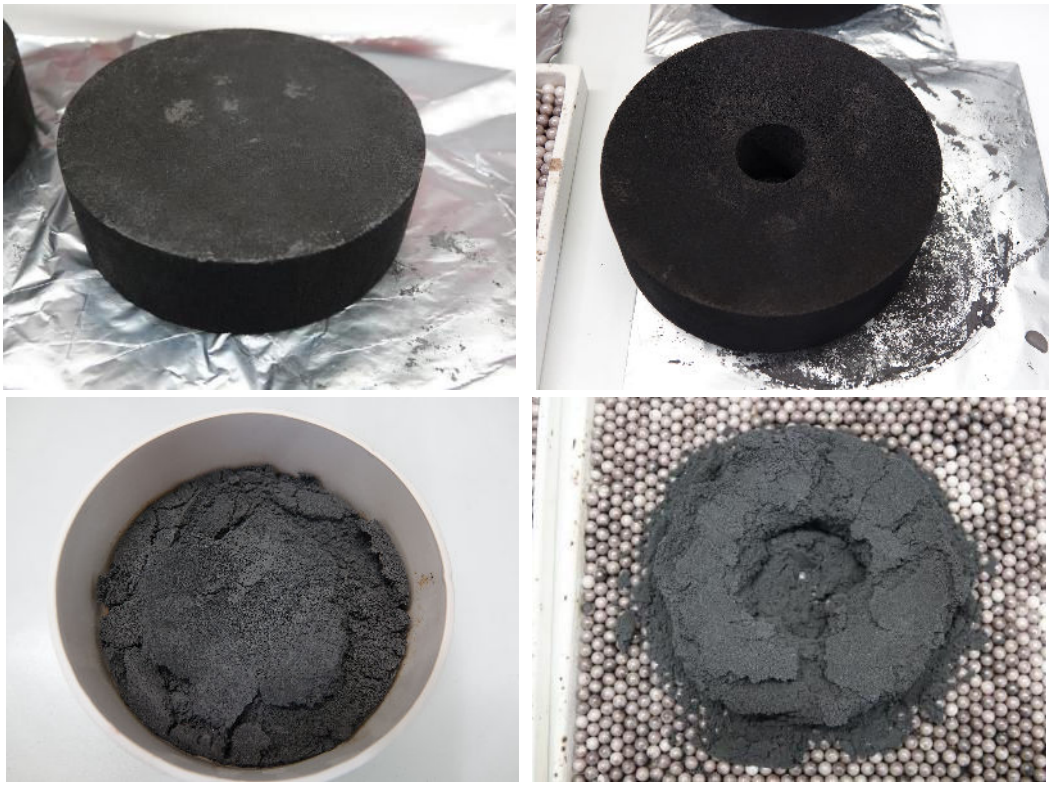

**Figure 1:** Representative images of the outcome of the scaling-up attempts of foam-like structures prepared by the PU-templating method. Photographs of impregnated PU templates of Ø 135 mm (top row) and perovskite foams made out of them that collapsed (bottom row).

Evidently, the outcome was not successful for the larger scale structure. Contrary to the small ones (see deliverable D3.1), the larger structures collapsed almost completely thereby indicating that scaling-up of foam-like redox structures is very challenging. This

is most likely due to insufficient coating of the template, especially in the radial direction (i.e. towards its central area). Consequently, the relatively low amount of redox material is unable to maintain the structure's integrity after burning/removal of the polymeric template that takes place during the firing up to 1300°C step. Currently, attempts to improve the coating process are underway at DLR but the problem has not been solved yet. Thus, as of the date of submission of the present deliverable, the scaling-up manufacturing feasibility of foam-like structures was not favored.

### 2.3.2 Extrusion of redox honeycombs

Regarding extrusion, an initial main challenge for scaling-up relates to the relatively high amount of redox powder required to proceed with the relevant necessary tests and subsequent optimization process to achieve manufacturing of larger structures. Such larger structures were initially defined for cylindrical honeycombs of ∅ 80-120 mm x up to 175 mm in length (indicatively). It was considered that such sizes, especially in term of cross-sectional increase, are adequate to assess scaling-up feasibility perspectives and already constitute a major step forward compared to the ∅ ~26 mm honeycombs manufactured so far by WP3. Naturally, other configurations should not be excluded as a next step and for final implementation of the WP5 system. Taking into account the requirements for the aforementioned scaled-up structures, a quantity of redox powder in excess of 50 kg was assessed as necessary. To address this challenge, it was decided to proceed with the extrusion of a homogeneous mixture of commercially procured raw powders and subsequent drying and high temperature (1200-1300°C) calcination of extruded honeycombs. The targeted composition, also considering experimental results so far, is CS10MO ($Ca_{0.90}Sr_{0.10}MnO_3$), which means that the required raw powders are $CaCO_3$, $Mn_3O_4$ and $SrCO_3$ mixed in stoichiometric quantities to form a homogeneous mixture. In-principle, such an approach has certain advantages but there are also challenges to be considered and tackled:

- The evolution of substantial amounts of $CO_2$ during calcination of the two carbonate salt precursors may be detrimental to the structural stability of the final fired structure as this evolution happens through the whole mass of the extruded body and takes place in the general temperature range of 600-900°C; i.e. well below the maximum temperature of 1200-1300°C that is expected to ensure sintering of the honeycomb. To put this phenomenon into perspective, the stoichiometric mixture loses approximately 24.3 wt% of its initial mass during dissociation of both $CaCO_3$ and $SrCO_3$ whereas the typical total mass of organics contained in an extruded dried green body is well below 20 wt%. Summing up both, it is evident that the total mass loss in the firing step may reach 40 wt% or more of the mass of the initial dried green body.
- The above issue points towards designing a complex and time-consuming calcination protocol that will allow the controllable removal of evolved gases so

that the final structure retains its structural integrity and is obtained as a robust structure.

- As a result of the above, it is highly likely that the final obtained structures will be more porous as compared to the calcination of extruded pre-synthesized CS10MO, which will result to a lower bulk density, thereby decreasing its total volumetric energy density potential (see also explanations earlier in the text and D3.2).
- On the other hand, a main advantage is that performing synthesis and calcination of structures in one step, instead of pre-synthesizing the CS10MO powder via calcination to promote the solid state reaction, milling the heavily sintered perovskite powder to the fine size required for preparation of the extrusion mixture, extruding and re-calcining to sinter the structure, can save significant amounts of energy and associated $CO_2$,eq emissions (see also section 2.4 below for more details).

Experimental validation for the tackling of the above challenges started with small-scale extrusion at CERTH using a thoroughly mixed and homogenized mixture of 2 kg of raw powders ($d_{50}$ < 5 μm and $d_{90}$ ~ 22 μm). The main aim was to have a first assessment of the extrudability of the mixture and most importantly to validate whether the structures can actually survive the substantial evolution of gases (i.e. mainly $CO_2$ due to dissociation of carbonate raw powders but also in combination from burning of organic additives) and be robust enough after high temperature calcination. Comparison to extrusion tests so far with pre-synthesized CMO-based honeycombs are also important. Figure 2 shows representative photographs from such honeycombs in their green and calcined (at 1200$^o$C) form. For the 59 cpsi honeycomb geometry, an additional photograph of a structure calcined according to a non-optimal protocol is also included (Figure 2e) to stress out the fundamental importance of defining an appropriate calcination strategy, especially for the case in question in which substantial $CO_2$ gas is also involved on top of the standard organic additives. Evidently, the tests were successful and provided initial confidence that the approach is feasible as the obtained honeycombs were in good condition and free of any major flaws (contrary to the case of Figure 2e honeycomb).

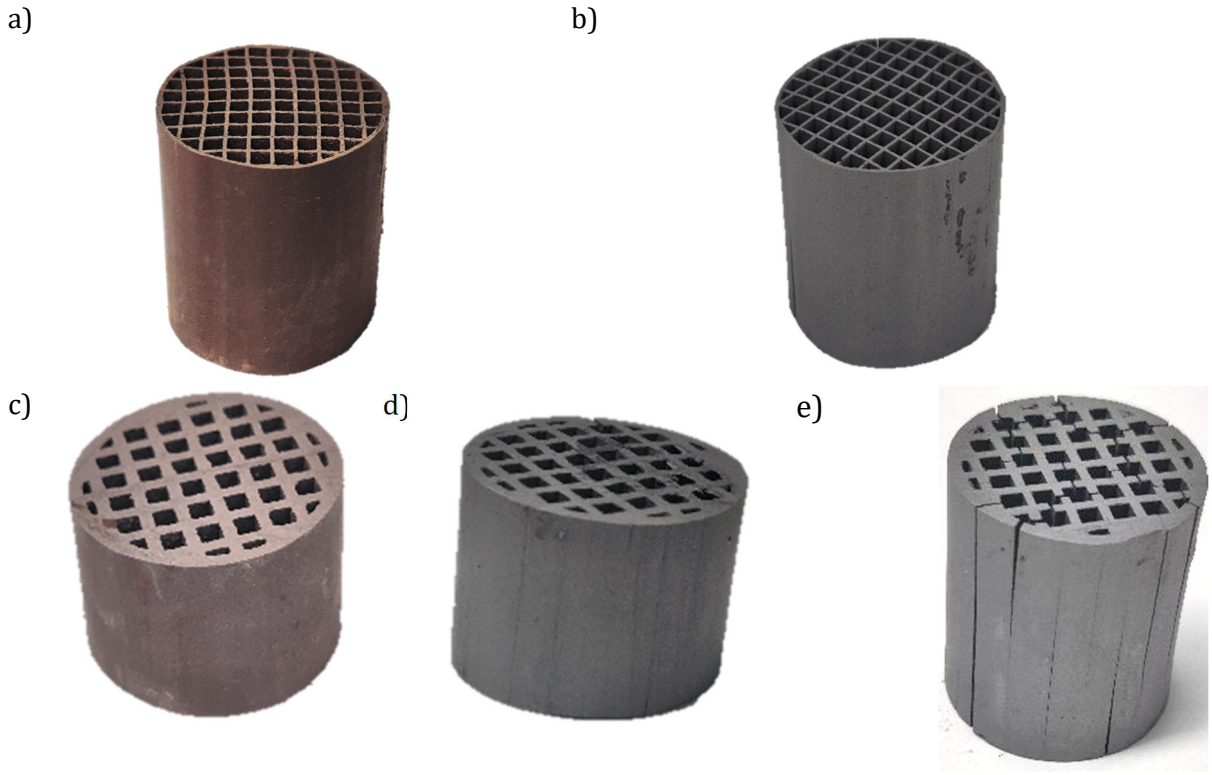


**Figure 2:** Indicative images from green and calcined extruded honeycombs from the raw powder mixture at CERTH: **a)** raw segment extruded with the 90 cpsi die; **b)** calcined segment from a) at 1200°C following the optimized calcination protocol; **c)** raw segment extruded with the 44 cpsi die; **d)** calcined segment from c) at 1200°C following the optimized calcination protocol; **e)** calcined segment from c) at 1200°C, following a non-optimized calcination protocol, in which numerous cracks are evident

As a next step, LET proceeded with the first scaling-up tests. 100 kg of a homogeneous mixture of raw powders (see earlier in the text) were prepared. The main equipment used for the scaled-up tests at LET (still ongoing at the time of submission of this deliverable) is shown in Figure 3.

As a starting point at LET and following the definition of an in-house developed protocol to achieve a good quality paste preparation (also based on CERTH's input from previous work described above), a ∅ 25 x 1000 mm flow-through geometry was extruded. As shown by the photographs of Figure 4 the test was successful. The dried green bodies were of high quality and free of defects. As of the time of submission of the present deliverable the work at LET is still ongoing but results so far on the scaling-up perspectives of the extrusion of redox bodies are encouraging and favorable. The first solid results that will also define the final feasibility of the approach are expected in the end of M28.

a) b)

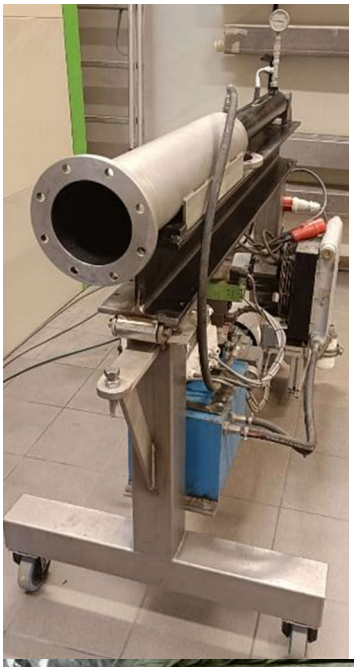

c) d)


**Figure 3:** Equipment used for the scaled-up extrusion tests at LET: a) mixer for the preparation of the extrudable past; b) Piston extruder; c) purpose-built table for receiving the structured body as extruded; d) ∅ 80 mm, 90 cpsi extrusion die to be used for the initial scaled-up extrusion tests

a)

b)

c)

**Figure 4:** Green bodies from the preliminary scald-up extrusion tests at LET. The pictures present extruded segments from a ∅ 25 mm die for the preparation of flow-through membranes at LET

Following the above mentioned work on preparatory and first scaling-up feasibility assessment, LET proceeded with the extrusion of larger honeycombs using the equipment and tools shown in Figure 3 above. This upscaled extrusion for the initially targeted geometry of ∅ 80 90 cpsi was successful, as demonstrated in the photographs of Figure 5 below. Some minor issues with uneven skin were identified but this is a common phenomenon for the case of newly developed extruded materials and will be fixed by additional tests and more precise control of extrusion parameters.

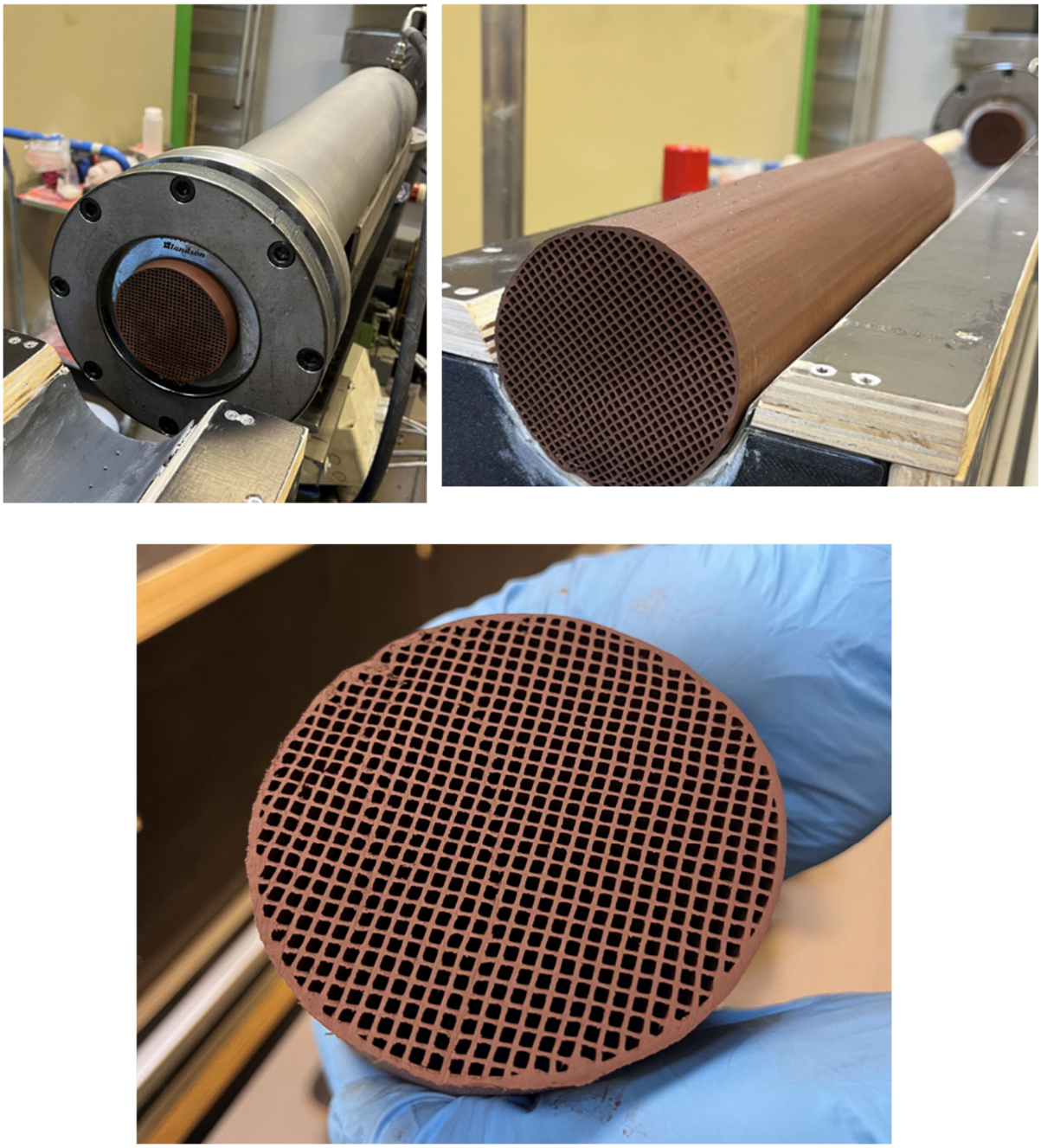

**Figure 5**: Indicative photographs from the first extrusion campaign at LET to produce larger honeycombs of ∅ 80 mm 90 cpsi geometry. Honeycombs are shown as received from extrusion and prior to drying

Regarding the drying process, only preliminary work has been carried out by the time of preparation of this deliverable. As shown in Figure 6, the abovementioned minor issues of as-received extruded bodies are somewhat magnified in the dried honeycomb. It is, however, evident that these issues are not detrimental and thus **the overall process so far**, especially considering the preliminary nature of tests presented here, **is assessed as successful**. The way to mitigate this issue during the whole process is to actually prepare a substantial amount of material mixed to properly adjust parameters like extrusion

speed, air table flow, drying strategy etc. LET is currently working towards this direction and results will be reported in WP5.

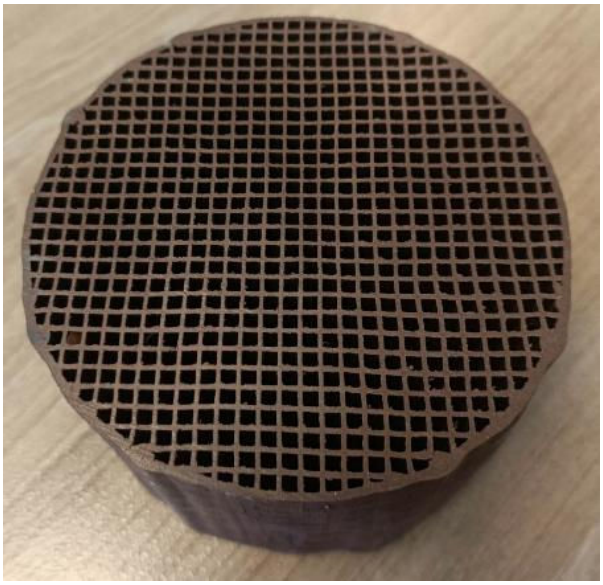

**Figure 6**: Representative photo of the cross-section of the honeycomb depicted in Figure 5 after the drying step (preliminary result).

### 2.3.3 Coating of inert substrates – fall back option

A safe fall-back option to the above challenging approach, currently evaluated at DLR, is the coating of suitable inert ceramic structures (e.g. cordierite honeycombs) with the same redox material. This is a straightforward technique, which has no risk and has been successfully applied in the past by members of the consortium in the RESTRUCTURE project [2]. Figure 7 shows characteristic stages of this procedure. Cordierite specimens of high cell densities, 400, 600 and 900 cpsi and of dimensions suited to fit in a metallic cartridge to be used in a reactor test rig for thermochemical evaluation of perovskite structures (see D3.1), were sectioned from commercial cordierite honeycombs used for substrates of automotive catalytic converters. The honeycombs were coated via the so-called "washcoating" technique also employed in automotive exhaust catalytic after-treatment , with different loadings of CSM10 powder in the range of 45-60 wt % (i.e. weight of coated powder)/(initial weight of dry support). The procedure comprises consecutive impregnations in a powder slurry, expulsion of the excess slurry from the channels by a blowing air stream, drying of the coated supports after each impregnation and a final calcination stage at 1150$^{o}$C to firmly adhere the coating onto the support. This last calcination temperature was selected on purpose to be higher than the upper limit of thermochemical cyclic tests (1100$^{o}$C) to ensure than no further sintering takes place during them. It is obvious that high loadings will increase the volumetric energy storage density of these structures; however, on the other hand high loadings might block a significant area of the channels available for gas flow and induce significant pressure

drop. Therefore, the coated specimens are measured with respect to their permeability vs. the non-coated supports in order to determine the optimum loading range that can ensure high energy density values simultaneously with acceptable pressure drop. Relevant information and data is provided below. Table 5 provides information on various uncoated cordierite samples and their corresponding mass and loading after their coating with CS10MO. This is an ongoing work, however results produced so far are enough to proceed with the first evaluation of this approach as explained below.

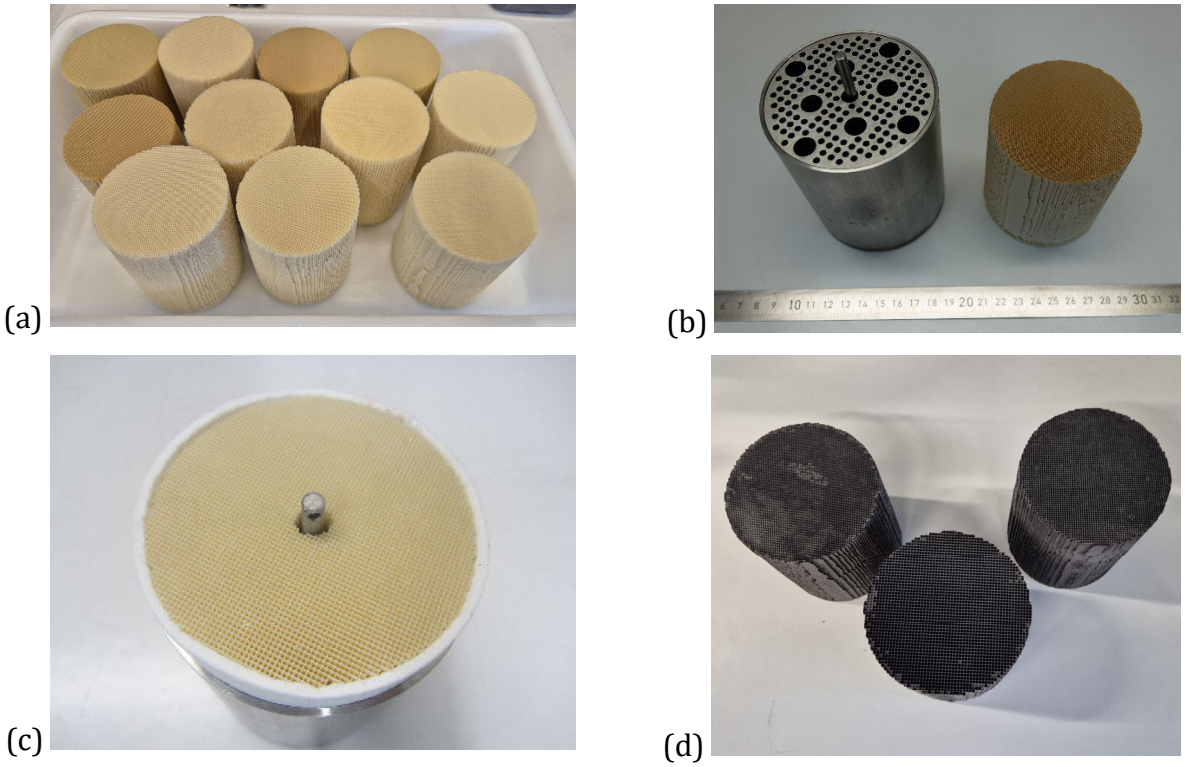

**Figure 7**: Sequence for preparation of perovskite-coated cordierite honeycombs: (a) cordierite specimens of 400, 600 and 900 cpsi, core-drilled from real-size pieces so that to fit into test reactor cartridge (b), after being drilled in the center (c); (d) 400, 600 and 900 cpsi CS10MO-coated specimens.

| Sample Code | Mass, uncoated segment | Mass after 1st coating | Loading (wt%) | Mass after 2nd coating | Loading (wt%) | Mass after 3rd coating | Loading (wt%) |
|---|---|---|---|---|---|---|---|
| **400 cpsi 1** | 109.67 g | 141.31 g | 28.9% | 166.76 g | 52% | | |
| **400 cpsi 2** | 110.34 g | 137.48 g | 24.6% | 157.89 g | 43% | 178.27 g | 61.6% |
| **600 cpsi 1** | 137.06 g | 171.00 g | 24.8% | 200.00 g | 46% | | |
| **600 cpsi 2** | 135.05 g | 163.56 g | 21.1% | 178.38 g | 32% | 218.00 g | 61.4% |
| **900 cpsi 1** | 103.40 g | 128.66 g | 24.4% | 163.00 g | 58% | | |
| **900 cpsi 2** | 103.31 g | 119.44 g | 15.6% | 139.80 g | 35% | 170.00 g | 64.6% |

**Table 4:** Loading of 400, 600 and 900 cpsi CS10MO-coated specimens.

It is obvious that high loadings will increase the volumetric energy storage density of these structures; however, on the other hand high loadings might block a significant area of the channels available for gas flow and induce significant pressure drop, especially when pressurized air streams are used. Therefore, the coated specimens were measured with respect to their permeability vs. the non-coated supports in order to determine the optimum loading range that can ensure high energy density values simultaneously with acceptable pressure drop.

Permeability reflects the ease with which a fluid flows through the voids of a porous medium. It is usually expressed by the parameters *k1* and *k2* derived from the Forchheimer equation (1) below. $\Delta P$ is the pressure gradient along the flow direction, μ and $\rho_f$ are respectively the dynamic viscosity and the density of the fluid, and V*s* is the *superficial* fluid velocity, determined by dividing the volumetric flow rate Q by the specimen area exposed to flow A. Parameters $k_1$ *and* $k_2$: *are known as the* viscosity and the inertial coefficient, respectively. In the case that frictional forces dominate the flow as for example in flow-through honeycombs with straight channels, the linear term of equation (1) has major contribution and the permeability coefficient (k) can be calculated from Equation (2). The quadratic term of equation (1) has major contribution, if inertial forces dominate the flow as for example in foams, where the flow has to follow the tortuous paths through the foam "megapores".

$$\frac{\Delta P}{L} = \frac{\mu}{k_1} V_s + \frac{\rho_f}{k_2} V_s^2 \quad (1)$$

$$k = \frac{\mu L U_0}{(P_i - P_0)} = \frac{\mu L Q}{A(P_i - P_0)} \quad (2)$$

Permeability measurements were carried out with an in-house built set-up at DLR. The operation principle, the device and the specimens are shown in the sequence of photographs in Figure 8. Air, at different values of gas flow rate (*Q)* varied through a mass flow controller, is blown via a fan through the porous specimen and the pressure difference between the outlet and the inlet is measured as a function of the air velocity. A typical graph of the pressure drop evolution per unit length as a function of the linear velocity of the applied flow rate for the so far measured non-coated and coated honeycombs is shown in Figure 8e. With respect to the non-coated supports, the trend is the expected one, since channels of smaller cross-section (i.e. in honeycombs of higher cpsi, induce higher pressure drop; in other words, it is more difficult for the fluid to flow through them. Furthermore, the coating, especially in the highest-cell-density honeycomb affects indeed adversely yet not critically the permeability. Measurements of the remaining specimens are in progress, in combination with preparation of specimens in the lower cpsi ranges but with even higher loadings.

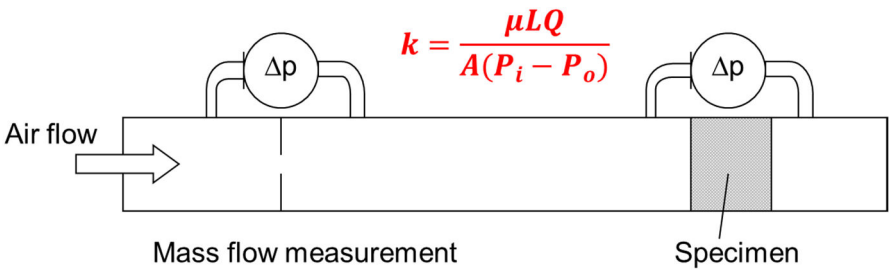


(a)

(b)

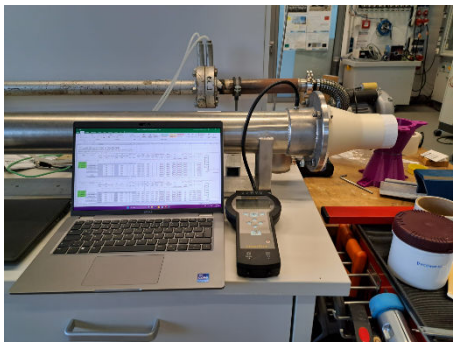

(c)

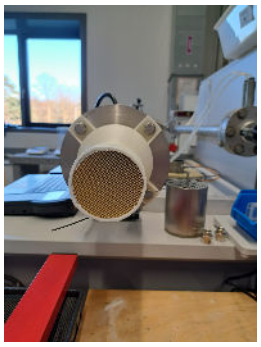

(d)

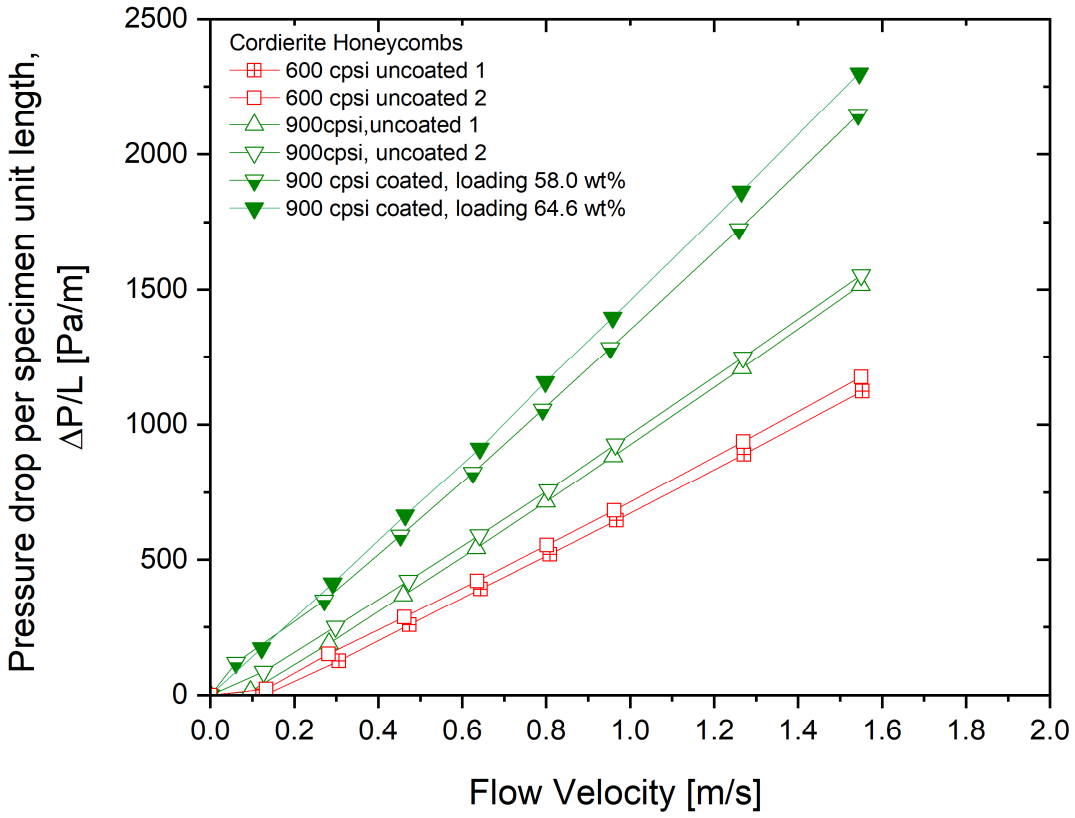


(e)

**Figure 8:** (a) Operation principle of in-house built permeability measurement device at DLR; (b) coated cordierite honeycomb specimens with their lateral surface sealed with a ceramic felt; (c), (d) side and front views, respectively, of specimen mounted at the device, ready for measurement; (d) typical graph of the pressure drop evolution per unit length as a function of the linear velocity of the applied flow rate for non-coated and coated 900 cpsi honeycombs.

It must be mentioned that, in addition to its obvious advantages, this coating approach has the inherent disadvantage of having a relatively low amount of redox material per reactor volume because the main portion of the mass is occupied by the inert substrate. This means that the thermochemical contribution to the overall energy storage density of the system will be lowered substantially compared to the current estimated 30% and therefore the total energy density will also decrease measurably. Thus, it makes sense to further pursue other approaches that aim at manufacturing the entire structure from the redox material itself (e.g. extrusion).

## 2.4 Preliminary environmental/financial aspects overview

As preliminarily identified by WP7 (see submitted deliverable D7.1), the calculated total carbon footprint of redox structures (i.e. honeycombs or foams) **when produced at laboratory scale** (i.e. up to a few kg of shaped material) is in the order of 9.2 – 10 kg $CO_2$-eq/kg of final product. Foam-like structures are positioned in the low end of this range and honeycombs at the high end of it but, in any case, the difference is small (< 10%) and thus the two approaches can be safely considered as essentially equivalent to each other in terms of their environmental impact. For both cases, major contributor with a share that exceeds 70% of total $CO_2$,eq emissions (and thus associated total energy consumption) are the necessary high temperature (~ 1300°C) calcination/sintering steps to achieve solid state synthesis of the perovskite and preparation of final structured body. By following, the modified protocol described above for **the synthesis of the perovskite and sintering of its structured form in one step** instead of two, the **carbon footprint decrease** at lab-scale manufacturing conditions is estimated to be **approximately 30%** and although currently followed for the extruded honeycombs case only, this is also in-principle applicable to the foam manufacturing process.

Scaled-up production, for which the project has not produced any data yet, is expected to decrease this footprint substantially but no relevant safe estimations can be made at the moment. Indicatively and as a rough approximation, a 5-10-fold decrease should be in-principle expected. Moreover, financial data is not yet available and relevant evidence is in fact expected to be produced in the frame of WP5 activities and specifically towards the final stage of implementation of that WP. However, it can be safely assumed that extrusion – being an already mature, large-scale, established and semi-automated process – is more financially favoured cf. the sacrificial PU-template manufacturing method, which has already found its near-commercial application in some niche sectors but it definitely lacks the maturity of extrusion.

Overall and from a combined preliminary environmental/financial viability point-of-view, it can be concluded that extrusion has a small advantage versus foam-like structures preparation via PU-templating.

## 2.5 Overall assessment & choice

The overall assessment and final choice is based on a multi-criteria semi-quantitative evaluation which is implemented in Table 5. The individual criteria are given a mark in the range of 1 (unacceptably low performance) to 5 (excellent performance) per structure evaluated in WP3 so far. The mark is given based on results available until M27 and its precise value may be relatively under- or over-estimated per case. However, and on a global comparative assessment (see total performance indicator value), the result can be considered as accurate, at least based on the outcome at hand by the time of submission of the present deliverable. Rather than using specific cpsi values for the case of honeycombs, a qualitative differentiation between ''high'' and ''low'' cpsi values is used in Table 5 to show the trend.

| Structure | High cpsi CMO honeycomb | Low cpsi CMO honeycomb | CS10MO foam | Low cpsi CS10MO honeycomb |
|---|---|---|---|---|
| **Energetic performance** | 2.5 | 4 | 2 | 5 |
| **Structural robustness** | 1.5 | 2 | 3 | 4 |
| **Manufacturing scalability** | 4 | 4 | 3 | 4 |
| **Preliminary environmental & financial aspects** | 3 | 3 | 2.5 | 3 |
| **Heat exchange efficiency** | 3 | 2 | 5 | 2 |
| **TOTAL performance indicator** | **14** | **15** | **15.5** | ***18*** |

**Table 5:** Overall performance of small-scale redox structures studied so far with respect to the 4 main aspects defining their suitability to the ABCSPF's application. *Allocated marks are in the scale of 1 (unacceptably low performance) to 5 (excellent performance)*

The highest overall mark is calculated for the case of **the low cpsi CS10MO honeycomb** as this structure combines excellent energy density/energetic performance with very good structural robustness and in-principle excellent manufacturing scalability potential. Its heat exchange efficiency, due to its relatively low surface area compared to the other structures, is relatively low but in a larger scale reactor it is believed that this can be mitigated via proper design measures and regulation of operating parameters (e.g. gas flow per reactor volume to ensure maximum efficiency of heat transfer).

# 3. Conclusions

The analysis of all parameters to be considered for the current assessment and choice of **most favourable route for scaling-up** the manufacturing of redox structured bodies, at least up to a scale able to meet the general requirements of the prototype systems to be implemented and operated in the framework of WP5 and WP6, **points towards extruded honeycombs** and preferably at a geometry of relatively low cpsi value that will ensure a relatively high bulk density to ensure sufficient volumetric storage density. On the other hand, the heat exchange efficiency must be also ensured and thus it is really difficult to precisely define the final geometry of choice at this stage. **Considering the available extrusion tools at LET, the starting point is a geometry of ∅ 80 mm and 90 cpsi** (nominal die value). For this geometry **first extrusion and drying tests were successful** and currently work towards optimisation and resolution of minor issues identified is underway. Calcination tests have not been carried out yet. DLR will test these honeycombs at a reactor of an intermediate size (i.e. size between the final prototype – currently under design – and the small-scale test-rig used by CERTH in WP3) and the results will be used to define the geometry more accurately. A new extrusion tool (e.g. of lower nominal cpsi) will be designed and constructed, if deemed necessary, considering the outcome of tests at DLR. At the same time, **coating of inert (i.e. cordierite) flow-through honeycombs** with the redox material, considered as a fall back option to preparing all-redox structures, **has been successful**. First permeability results indicated that the pressure drop through the structures was within acceptable values and the addition of coating (loadings up to > 50% loading of redox material) did not induce appreciable resistance to the gas flow.

# 4. References

[1] G. Karagiannakis, C. Pagkoura, E. Halevas, P. Baltzopoulou, A. G. Konstandopoulos, Cobalt/cobaltous oxide-based honeycombs for thermochemical heat storage in future concentrated solar power installations: Multi-cyclic assessment and semi-quantitative heat effects estimations, Solar Energy, 133, 394-407 (2016).

[2] G. Karagiannakis, C. Pagkoura, A. G. Konstandopoulos, S. Tescari, A. Singh, M. Roeb, M. Lange, J. Marcher, A. Jové, C. Prieto, M. Rattenbury, A. Chasiotis, Thermochemical storage for CSP via redox structured reactors/heat exchangers: The RESTRUCTURE project, AIP Conference Proceedings, 1850, 090004-1 – 090004-9 (2017).